Appl. Phys. A 91, 1–5 (2008)
DOI: 10.1007/s00339-007-4394-x

Applied Physics A
Materials Science & Processing

Invited paper

V.J. LOGEESWARAN[1]
A. SARKAR[1]
M.S. ISLAM[1,✉]
N.P. KOBAYASHI[2]
J. STRAZNICKY[3]
XUEMA LI[3]
WEI WU[3]
SAGI MATHAI[3]
M.R.T. TAN[3]
SHIH-YUAN WANG[3]
R.S. WILLIAMS[3]

A 14-ps full width at half maximum high-speed photoconductor fabricated with intersecting InP nanowires on an amorphous surface

[1] Department of Electrical and Computer Engineering, University of California at Davis, Davis, CA 95616, USA
[2] Jack Baskin School of Engineering, University of California at Santa Cruz, Santa Cruz, CA 95064, USA
[3] Quantum Science Research, Advanced Studies, Hewlett-Packard Laboratories, Palo Alto, CA 94304, USA

Received: 13 December 2007 / Accepted: 14 December 2007
Published online: 29 January 2008 •

ABSTRACT We demonstrate a high-speed polarization-insensitive photoconductor based on intersecting InP nanowires synthesized between a pair of hydrogenated silicon electrodes deposited on amorphous SiO_2 surfaces prepared on silicon substrates. A 14-ps full width at half maximum de-embedded impulse response is measured, which is the fastest reported response for a photodetector fabricated using nanowires. The high-speed electrical signal measurements from the photoconductor are performed by an integrated coplanar waveguide transmission line. The demonstrated ability to grow intersecting InP nanowires on hydrogenated microcrystalline Si surfaces will facilitate the construction of ultra-fast photodetectors on a wide range of substrates.

PACS 61.46.Km; 42.70.-a; 81.16.Hc; 81.05.Ea; 85.60.Dw

1 Introduction

For more than four decades, advances in high-speed semiconductor photodetectors were driven by emerging fiber optical communication systems [1–4]. III–V materials were at the center of this development due to their direct band gap properties which ensure high absorption coefficients resulting in device structures that allow operations in the tens and even hundreds of GHz in bandwidth. Due to silicon's inability in efficient generation and high-speed detection of near-IR photons used in telecommunications, the integration of large areas of high-performance III–V materials with Si technology has been mainly pursued using methods such as wafer bonding [1, 8], hetero-epitaxy [5, 6], and epitaxial lift-off [7]. The advantages of such an integration of III–V materials to silicon are numerous. For example, the integration of photonic devices such as optical sources, modulators, and detectors is essential to provide electronic-to-optical (E/O) and optical-to-electronic (O/E) conversions using monolithically integrated electronic–photonic circuits where the information processing is done primarily relying on electrons and the majority of the information transfer is accomplished using photons.

Recently, the bottleneck in data-processing bandwidth at the board-to-board, chip-to-chip, and intra-chip level in computer data centers has re-intensified the desire to use photons for data transmission. A near-term goal of realizing inter-chip interconnects for computer servers and microprocessors has also gained enormous technological momentum. Low noise, small physical size, and the ability to assimilate with mainstream silicon electronics in large numbers are some of the desired features for a photodetector that will serve the requirements for future chip-to-chip and on-chip interconnects. Existing optical communication detectors are constrained by these requirements. One key technical challenge in implementing dense optical interconnects is to design a low-latency photodetector with a small capacitance to minimize amplifier gain stages and receiver noise [9]. The success of these efforts will depend not only on photon generators and detectors integrated on Si, but also on the usage of inexpensive substrates such as quartz, glass, and printed circuit boards (PCBs).

Among various III–V materials for Si integration techniques, high-quality epitaxial growth of planar layers of III–V compound semiconductors on Si substrates remains challenging because of material incompatibilities, such as large lattice and thermal expansion coefficient mismatches and differences in crystal structure [10, 11]. However, to circumvent the lattice and thermal mismatches, the use of semiconductor nanowire heterostructures was found to be effective due to the small dimensions of the nanowires (NWs). A number of highly crystalline III–V nanowires were recently grown on Si wafers with lattice mismatch as high as 8.1% [12–14]. These direct band gap semiconductor nanowires can offer high gain for designing laser diodes as well as superior absorption characteristics needed for high-speed photodetection. Several research groups have demonstrated nanowire-based photodetectors with a few GHz bandwidth responses [15, 16]. However, the challenges in manipulation and positioning the nanowires for device construction, high contact resistance, and difficulty in the integration of high-speed transmission lines with the current pick-and-place approach resulted in poor performances compared to existing commercially available photodetectors.

✉ Fax: +1-530-752-8428, E-mail: saif@ece.ucdavis.edu

In this paper, we introduce a new method of incorporating III–V nanowires on a non-single-crystalline surface that directly relaxes any lattice-matching conditions and report the demonstration of a device for high-speed photodetection based on InP nanowires grown in the form of nanobridges [12, 17] between prefabricated electrodes of hydrogenated microcrystalline silicon (μc-Si:H) deposited on an amorphous SiO_2 surface [18]. The device was characterized to have a de-embedded temporal response of 14 ps full width at half maximum (FWHM) when triggered by a 780-nm laser pulse.

2 Device fabrication

Figure 1a and b depict an illustration of our nanowire photoconductive device integrated on a high-speed coplanar waveguide (CPW) transmission line with 50-Ω characteristic impedance to facilitate DC and high-frequency measurements. The high-speed photoresponse signal is extracted through a CPW microwave probe (Cascade Microtech GSG-50). Figure 1c depicts the top view of a scanning electron microscope (SEM) image of the device and the photoactive region of the device is shown in Fig. 1d. A close-up illustration of the active photoconductive region is shown in Fig. 2a–d, which consists of a number of intersecting InP nanowire photoconductors over a 2-μm gap. The fabrication started with a 3-nm Ti film and a 100-nm Pt film for the CPW deposited onto a 2-μm thermally grown silicon dioxide (SiO_2) surface on a silicon substrate by vacuum thermal evaporation at ambient temperature. Subsequently, a 500-nm n-type hydrogenated silicon (n-Si:H) film (phosphorus-doping concentration $\sim 1 \times 10^{20}\,\mathrm{cm}^{-3}$) was deposited by plasma enhanced chemical vapor deposition (PECVD) onto the patterned Pt/Ti electrodes at 220 °C with source gases of silane (SiH_4), hydrogen, and phosphine (PH_3). This was followed by patterning the n-Si:H film, leaving the two segments of n-Si:H electrically connected to the Ti/Pt electrodes only in the active photodetector regions. A suspension of colloidal gold nanometer-scale particles (Au nanoparticles with nominal diameter of 10 nm) in toluene was used to uniformly coat the sample. Finally, InP was deposited by low-pressure metalorganic chemical vapor deposition (LP-MOCVD) on the processed wafer. InP grew into randomly oriented InP nanowires formed selectively onto the n-Si:H segments as shown in Fig. 1d. The random orientation of the nanowires is caused by the lack of crystallographic translational symmetry on the surface of the n-Si:H film. A large number of nanowires are found to grow towards the opposite n-Si:H segments and mutually 'weld', establishing an electrical continuity over the gap between the two n-Si:H segments. Despite coating the whole sample with colloidal gold nanoparticles, nanowires grew only on the n-Si:H segments suggesting a precondition of definite short-range atomic ordering for a coherent growth of nanowire heterostructures. Detailed characteristics of the material growth are reported in [18].

Contacts between a nanowire and an electrode and between two self-welded nanowires always possess a finite magnitude of resistance at the interface. This resistance contributes to enhanced Joule heating, higher circuit noise, and high RC time and thus degrades the system performance. For nanowires with small diameters, the contact resistance could be comparable with the nanowire resistance unless a scheme is employed for ensuring low contact resistance. Although metals make high-quality ohmic contacts to semiconductor thin films, they are found to contribute to a Schottky barrier when contacts are formed to nanowires [19]. We carried out a systematic characterization of self-welded nanowires between Si electrodes and measured a very low specific contact resistance of $5.02 \times 10^{-6}\,\Omega\,\mathrm{cm}^2$ for bridged Si nanowire interfaces [17]. This value is more than two orders of mag-

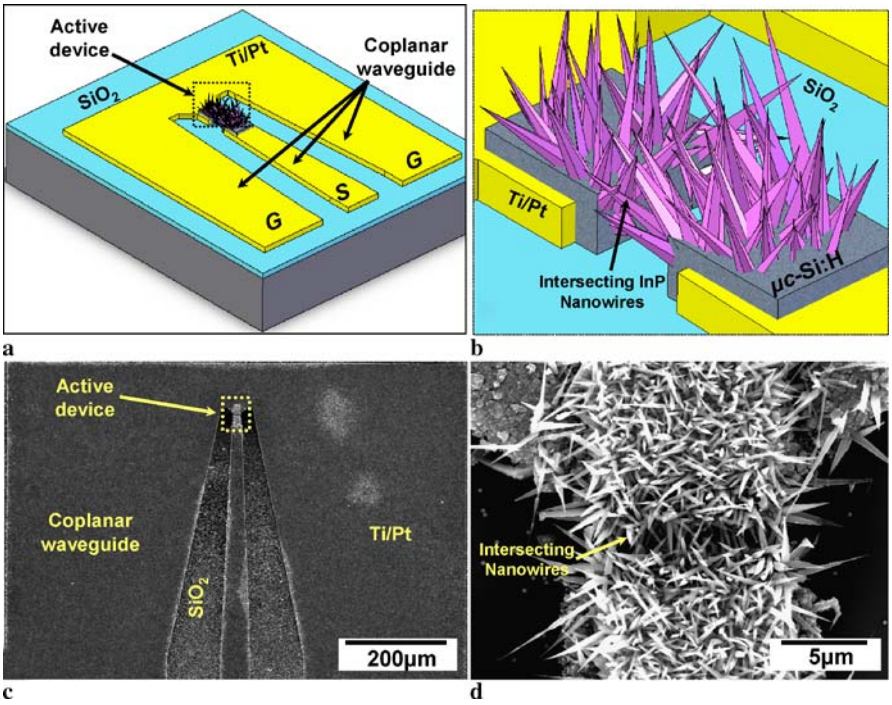

FIGURE 1 **a** Illustration of the InP-nanowire high-speed photoconductor, **b** a close-up view of the intersecting nanowire photoconductors, **c** SEM image of the entire device, **d** active region of the device

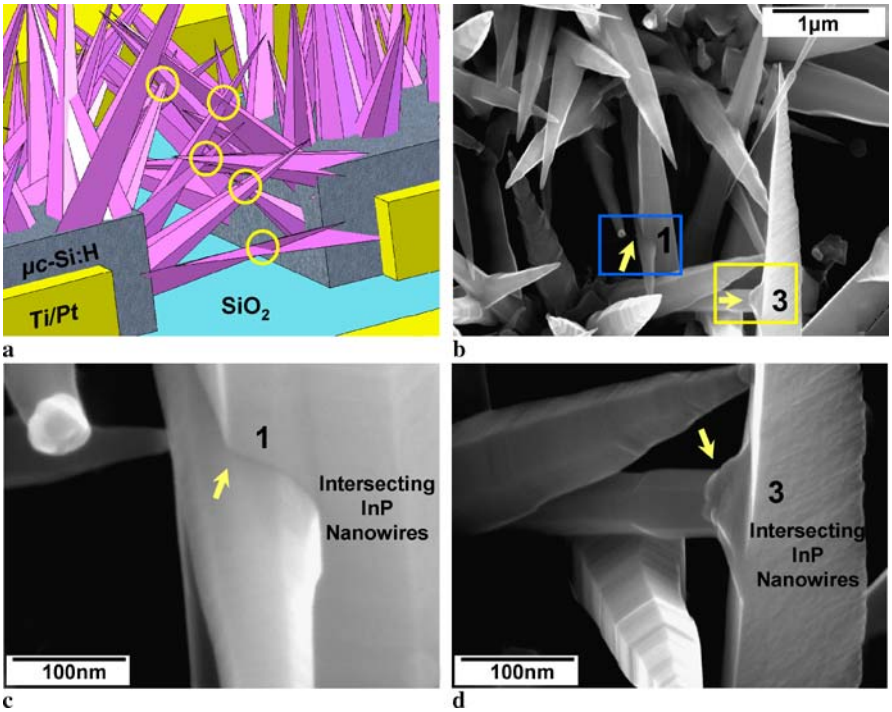

FIGURE 2 **a** Illustration of the intersection of nanowires across the two separated microcrystalline hydrogenated silicon electrodes of a high-speed photoconductor, **b** a close-up SEM view of the intersecting nanowire photoconductors, **c**, **d** magnified images highlighting the nanowire intersection indicated by *arrows*. The bridged gap is 2 μm

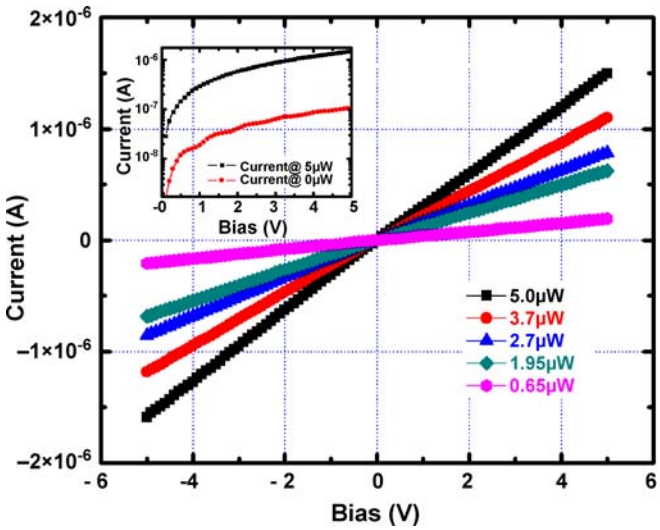

FIGURE 3 Linear current–voltage characteristics of the photoconductor with an active area of 10 μm × 2 μm for 5 μW, 3.7 μW, 2.7 μW, 1.95 μW, and 0.65 μW of input optical power at 633 nm. The *inset* shows the dark current and *I–V* characteristic for 5-μW illumination power in log–linear scale. At 5 V, the device exhibits a low dark current of ∼ 100 nA

nitude better than what was reported for Ti/Au contacts to Si nanowires [20]. The results of our highly linear and low-resistance ohmic contacts are the basis of implementing bridged and self-welded nanowires for designing the devices reported in this paper. It is evident from the *I–V* curves of Fig. 3 and the reported results in [17] that the welded contacts are ohmic in nature.

In a photodetector, the ultimate limit to the detectability of weak signals is set by the noise that obscures the desired signal in a communication link. This noise is the random fluctuating component of a voltage or current in a device, which can be caused by different mechanisms, for example carrier-mobility fluctuation and carrier trapping–detrapping. The noise property of modern nanoscale devices is even more important because they typically operate at a lower voltage, so the signal-to-noise ratio (SNR) is critical. We previously reported the characterization work on the $1/f$ noise of welded nanowires and compared it with that of carbon nanotubes (CNTs) and nanowire-based devices fabricated using the existing research-based interfacing method (metal evaporation on nanowires) [21]. Although it was widely speculated that the carbon nanotubes would be relatively less 'noisy' owing to their stable carbon–carbon bonds [22], our results show that on the contrary they are very noisy. Similarly, the noise level of conventional nanowire devices was also found to be very high. However, the noise level in our self-welded nanowires was found to be at least two orders of magnitude better than that of CNTs and nanowire devices [21]. The superior characteristics were the result of the highly epitaxial bonding or welding between two nanowires and nanowires–electrodes. These results substantiate our endeavor for employing the bridging/welding techniques for designing nanowire-based electronic and photonic devices.

3 Experimental results and discussions

The room-temperature direct current–voltage measurements were done by illuminating only the active photodetector area (10 μm × 2 μm) with a continuous-wave (CW) 633-nm laser source. Without laser illumination, the photoconductor was in a high-resistance 'off' state (∼ 50 MΩ). The dark current of the devices with a 10 μm × 2 μm intersecting InP nanowire region was measured to be ∼ 100 nA at 5 V. Upon laser illumination, the nanowire photoconductor is transformed into a lower-resistance state with its 'on'-state resistance dropping to ∼ 3 MΩ. The measured DC responsivity at 5 V is ∼ 0.3 A/W. Most of the devices

we measured demonstrated very linear current–voltage (I–V) characteristics typical of a photoconductor, as shown in Fig. 3. Slight nonlinearities resembling back-to-back rectifying diodes were observed in a number of devices and we attribute this to probable residual barriers in the contacts between the nanowires and the Si:H. Under optical illumination, the nonlinearities gradually disappeared with increasing input optical power, indicating a photo-induced surmounting of the contact barriers. At 5-V bias, the increase in current is more than an order of magnitude over the dark current with a coupled optical power of 5 μW to the active-device region. More than 99% of the change in resistivity is attributed to the InP NWs and a very negligible fraction is attributed to n-Si:H. Detailed analysis is presented in [23]. A discernable persistent photoconductance (PPC) was also observed during the DC measurement. We measured the dark current of the devices subsequent to illumination measurements and found the photogenerated excess carriers to recombine very slowly over a considerable time interval. This persistent photoconductance took a significant time to decay to the dark-current level, which was below 100 nA in most of our devices. The long recombination time is most likely caused by traps in the n-Si:H electrodes.

For the high-speed AC photoconductance characterizations, we used a pulsed laser source from a mode-locked fiber laser (Calmar Optcom) having a wavelength of 780 nm, a total output power of ∼ 90 μW, a pulse width of 1 ps, and a repetition rate of 20 MHz. The laser pulse was focused from the top surface by using free-space coupling onto the active region of the photoconductor using a single-mode lensed fiber tip on a microwave probe station. The resulting photoresponse electrical pulses were observed on a 40-GHz oscilloscope (Agilent 86109A). The center of the laser beam was aligned with a translational stage to maximize the photocurrent of a device within an area of 10 μm × 2 μm. We did not observe photosaturation in any of our devices and the photocurrent remained limited by the maximum power of our laser [23]. The overall error is expected to be within a few percent.

Figure 4 shows the measured pulse response when the device was biased at 1 V using a 45-GHz bias-T. The measured FWHM from the oscilloscope was 18 ps and considering the 11.2-ps FWHM response for the 40-GHz oscilloscope and the laser pulse width of 1 ps, the device temporal response was estimated to be 14 ps at 780 nm based on Eq. (1) of [24], which is given by

$$\tau_{\text{meas}} = \sqrt{\tau_{\text{actual}}^2 + \tau_{\text{scope}}^2 + \tau_{\text{optical}}^2}\,, \tag{1}$$

where τ_{meas}, τ_{actual}, τ_{scope}, and τ_{optical} are the measured, actual, oscilloscope, and optical pulse widths in time. This is acceptable for Gaussian pulses and is a good approximation for our actual measurements. Our estimate is conservative, since we have neglected the microwave components and laser timing jitter that contribute to the measured pulse width as well. The symmetrical shape of the temporal response suggested that the measurement was limited by the experimental setup. There is a residual photoconductance after the pulse fall time that caused a considerably long tail that may be mainly due to traps in the n-Si:H electrodes. These could be eliminated by shielding the electrodes from laser illumination in future device designs[1]. The unbiased DC capacitance of the device was measured to be ∼ 10–15 fF with an LCR meter (HP 4283) and hence does not limit the temporal response.

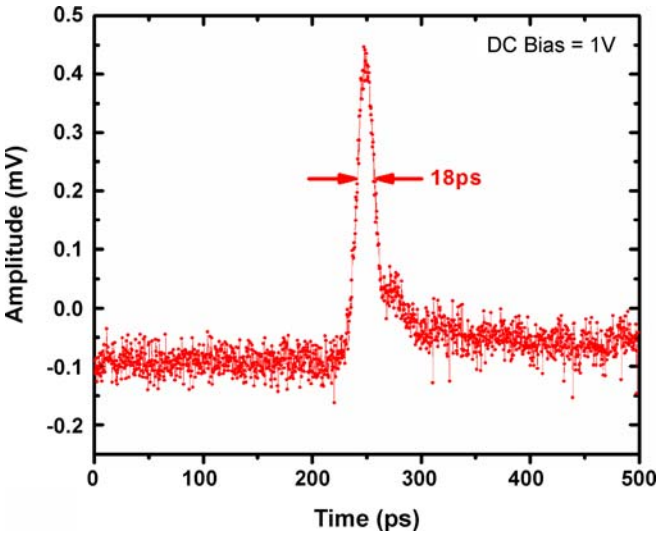

FIGURE 4 Measured high-speed pulse response of the InP-nanowire photoconductor with a 40-GHz Agilent oscilloscope triggered by ultra-short 780-nm laser pulses of width 1 ps. The device was biased at 1 V

A photon propagating through a fiber or free space carries a unique polarization in addition to its energy. A fundamental consequence is that nanowires oriented in a unique direction will vary in their coupling efficiency for different polarizations of photons (larger photocurrent for light polarized parallel to the wire than for light polarized perpendicular to the wire). In our device, randomness in the orientation makes them less sensitive to this and we observed less than 1 dB variation for different polarizations of light.

Anti-reflective (AR) coatings are commonly used in planar photodetectors to suppress reflection that generally contributes to lower quantum efficiency. Unlike the flat surfaces that are illuminated in a regular photodetector, nanowire-based devices offer the potential for trapping the incident photons by multiple reflections in the dense network of nanowires until they are completely absorbed. The optical spectral reflectance of an InP-nanowire-coated (100)-oriented GaAs sample and a reference GaAs substrate without the InP nanowire is graphed in Fig. 5. On (100)-GaAs, InP nanowires grew along two equivalent (111) directions of the substrate and show a dramatically reduced reflectance over the spectral range from 400 nm to 1150 nm even without using any AR coating. On n-Si:H electrodes, InP nanowires grew with a high degree of randomness in their orientations and can offer an intrinsic capability for significantly reduced reflection loss.

Future chip-scale photonic interconnects will demand ultra-fast Si-compatible photodetectors with ultra-low capaci-

[1] Our previous study indicated that the wavelength corresponding to the band-gap energy of the InP nanowires is in the range of 850–875 nm at room temperature [18]. The wavelength corresponding to the band gap of n^+-Si:H, on the other hand, is in the range of 620–688 nm according to a series of published literature. Hence, the device high-speed response with 780-nm pulsed illumination to which the n^+-Si:H should be transparent essentially is showing the photocurrent of InP nanowires.

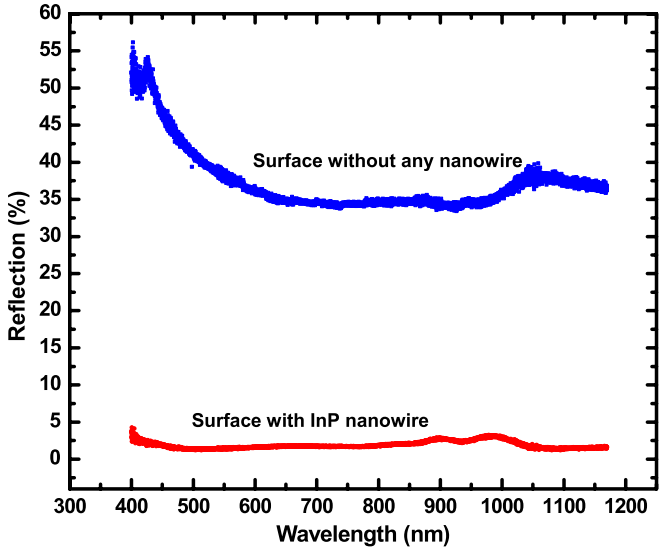

FIGURE 5 Optical reflectance of a bare surface and an InP-nanowire-coated surface. A nanowire-coated (100)-oriented GaAs surface shows greatly reduced reflectance over the spectrum ranging from 400 nm to 1150 nm. A Si surface with higher degree of randomness in the orientation of the nanowires is expected to be more effective in trapping photons than an anti-reflective (AR) coating

tance. In a miniaturized photodiode, the speed limit is likely to be constrained more by the RC time constant than the transit time. Despite offering high surface-to-volume ratio that helps in enhanced absorption of photons, NWs have very small total cross-sectional areas contributing to low junction capacitance. We measured capacitance–voltage characteristics of our devices as a function of the applied DC bias and found the capacitance to vary from 10 to 40 fF for bias voltages up to 2 V. The range of measured capacitance clearly demonstrates the potential for ultra-high-speed operation of the device. An opportunity for densely integrable high-speed nanoscale photodetectors could become a reality by employing III–V nanowires on Si surfaces along with the applications of plasmonic techniques that would miniaturize the device size as well as offering high responsivity [25].

4 Conclusion

In conclusion, we have demonstrated a high-speed polarization-insensitive photoconductor based on intersecting InP nanowires synthesized between a pair of hydrogenated microcrystalline silicon electrodes deposited on amorphous SiO_2 surfaces using a metal-catalyzed CVD process. Pulses with a FWHM of 18 ps were measured on the oscilloscope and have been estimated to represent a 14-ps FWHM de-embedded impulse response. Superior reflection-free absorption characteristics and ultra-low capacitance were also observed. The demonstrated ability to grow intersecting InP nanowires on microcrystalline Si surfaces is a step forward in the construction of ultra-fast photodetectors in III–V nanowires on a wide range of substrates.

ACKNOWLEDGEMENTS The work at UC Davis was partially supported by NSF Grant No. 0547679.

REFERENCES

1 J.E. Bowers, A.K. Srivastava, C.A. Burrus, J.C. Dewinter, M.A. Pollack, J.L. Zyskind, Electron. Lett. **22**, 137 (1986)
2 S.Y. Wang, D.M. Bloom, Electron. Lett. **19**, 554 (1983)
3 J.D. Schaub, R. Li, S.M. Csutak, J.C. Campbell, J. Lightwave Technol. **19**, 272 (2001)
4 L.Y. Lin, M.C. Wu, T. Itoh, T.A. Vang, R.E. Muller, D.L. Sivco, A.Y. Cho, IEEE Trans. Microwave Theory Tech. **45**, 1320 (1997)
5 E.A. Fitzgerald, Y.H. Xie, D. Monroe, P.J. Silverman, J.M. Kuo, A.R. Kortan, F.A. Thiel, B.E. Weir, J. Vac. Sci. Technol. B **10**, 1807 (1992)
6 J. Geske, Y.L. Okuno, J.E. Bowers, V. Jayaraman, Appl. Phys. Lett. **79**, 1760 (2001)
7 E. Yablonovitch, T. Gmitter, J.P. Harbison, R. Bhat, Appl. Phys. Lett. **51**, 2222 (1987)
8 L. Fotiadis, R. Kaplan, Appl. Phys. Lett. **55**, 2538 (1989)
9 D.A.B. Miller, Proc. IEEE **88**, 728 (2000)
10 H. Mori, M. Sugo, Y. Itoh, Adv. Mater. **5**, 208 (1993)
11 A. Krost, F. Heinrichsdorff, D. Bimberg, Appl. Phys. Lett. **64**, 769 (1994)
12 S.S. Yi, G. Girolami, J. Amano, M.S. Islam, S. Sharma, T.I. Kamins, I. Kimukin, Appl. Phys. Lett. **89**, 133 121 (2006)
13 T. Martensson, C.P.T. Svensson, B.A. Wacaser, M.W. Larsson, W. Seifert, K. Deppert, A. Gustafsson, L.R. Wallenberg, L. Samuelson, Nano Lett. **4**, 1987 (2004)
14 L.C. Chuang, M. Moewe, C. Chase, N.P. Kobayashi, C. Chang-Hasnain, S. Crankshaw, Appl. Phys. Lett. **90**, 43 115 (2007)
15 J.F. Wang, M.S. Gudiksen, X.F. Duan, Y. Cui, C.M. Lieber, Science **293**, 1455 (2001)
16 L. Luo, Y.F. Zhang, S.S. Mao, L. Lin, Sens. Actuators A **127**, 201 (2006)
17 A. Chaudhry, V. Ramamurthi, E. Fong, M.S. Islam, Nano Lett. **7**, 1536 (2007)
18 N.P. Kobayashi, S.Y. Wang, C. Santori, R.S. Williams, Appl. Phys. A **85**, 1 (2006)
19 M.H. Ham, J.H. Choi, W. Hwang, C. Park, W.Y. Lee, J.M. Myoung, Nanotechnology **17**, 2203 (2006)
20 S.E. Mohney, Y. Wang, M.A. Cabassi, K.K. Lew, S. Dey, J.M. Redwing, T.S. Mayer, Solid State Electron. **49**, 227 (2005)
21 S. Reza, G. Bosman, M.S. Islam, T.I. Kamins, S. Sharma, R.S. Williams, IEEE Trans. Nanotechnol. **5**, 523 (2006)
22 P.G. Collins, M.S. Fuhrer, A. Zettl, Appl. Phys. Lett. **76**, 894 (2000)
23 N.P. Kobayashi, V.J. Logeeswaran, X. Li, M.S. Islam, J. Straznicky, S.Y. Wang, R.S. Williams, Y. Chen, Appl. Phys. Lett. **91**, 113 116 (2007)
24 K. Rush, S. Draving, J. Kerley, IEEE Spectrum **27**, 38 (1990)
25 Z. Yu, G. Veronis, S. Fan, M.L. Brongersma, Appl. Phys. Lett. **89**, 151 116 (2006)